NUMERICAL MODELING AND EXPERIMENTAL INVESTIGATION OF LASER-ASSISTED MACHINING

ARTI OJHA
Research Scholar, Physics, Sangam Universty , Bhilwara
DR. ABHISHEK SAXENA
Assistant Professor, Physics, Sangam Universty , Bhilwara
DR. KAMAL CHAND JAIN
Professor, Physics, M.L.V.T.E.C, Bhilwara

ABSTRACT
In this research, we assess the damage that an Al2O3 ceramic coating sustained from a molten pool laser. Following a mechanism investigation of the laser damage, a 2D finite element model of laser ablation of the Al2O3 ceramic coating was developed. The unit included laminar flow, heat transport, and the level set approach of solid mechanics. The findings showed that melting, gasification, spattering, and microcracking were induced by laser ablation. The ablation depth and diameter increased with longer laser ablation times under continuous irradiation. There was consistency between the simulated and experimental profiles. Furthermore, since the laser ablation stress (3500–9000 MPa) was greater than the tensile stress (350–500 MPa), microcracks and fractures occurred. With the purpose of predicting the form of laser damage, COMSOL Multiphysics was used to conduct laser damage analysis, which verified the results of the 3D surface profiler and scanning electron microscope.

INTRODUCTION
An energy source is used to pump the active medium in every laser system. Usually, the active material is positioned between two strongly reflecting mirrors, one of which is optically parallel and the other partially transparent. The gain medium may be a solid, liquid, or gas that has the capacity to stimulate emission and increase the amplitude of light waves passing through it. Pumping can be accomplished electrically or optically. Before being released via the transmitting mirror, light bouncing between two mirrors would first pass through the gain medium, which would magnify it. Optical amplifiers were designed using this configuration.
Consider a medium whose atoms may only be in one of two states: ground (E1) or excited (E2). After being aroused to the upper state (E2) by any pumping mechanism (such as light, electricity, current flowing through, or electron bombardment), atoms in the ground state (E1) will quickly return to the E2 and produce photons with energy $hv = E2 \rightarrow E1$ in a matter of nanoseconds. Einstein postulated in 1917 that both photon-induced and spontaneous emission processes are plausible.

We have induced emission in the first scenario and spontaneous emission in the second. The stimulated emission photons constructively enhance the stimulating photon wave, increasing its amplitude and causing lasing, since their frequency, phase, and polarisation state are the same as the stimulating photon's. Because there is a far lower chance of stimulated emission than spontaneous emission, the majority of conventional light sources are incoherent while they are operating at thermal equilibrium (1: 1033). Lasing is only practical when working outside of thermal equilibrium.

Modification in Basic Laser Structure

In order to generate integral multiples of the laser's frequency and alter the pulse width, shape, and energy/pulse, it is necessary to add electrical, optical, or electro-optical devices between the mirror and active media. This is crucial for advanced technological applications. Common techniques in modern laser technology include mode locking or phase locking, Q-switching, shaping pulses, compressing and expanding pulses, multiplying frequencies, and so on.

The outcome is an output pulse with a positively chirped1 (frequency rises with time) component because the lower-frequency one comes initially and the higher-frequency one comes relatively later. The opposite is true with planoconvex or biconvex lenses, which provide negative chirped output (longer route length for lower frequency) and shorter path length for higher frequency. The duration of the pulse, or the stretching of the laser pulse, may be increased by either positive or negative chirping. When the chirp is reduced or eliminated, the pulse is compressed, meaning its length is reduced.

1) When several parts of a laser pulse's frequency spectrum emit at different times, this phenomenon is known as chirping. "Positive chirping" occurs when the pulse's light components' frequencies rise with time, "negative chirping" occurs when they fall, and "un-chirped" occurs when their frequencies remain constant.

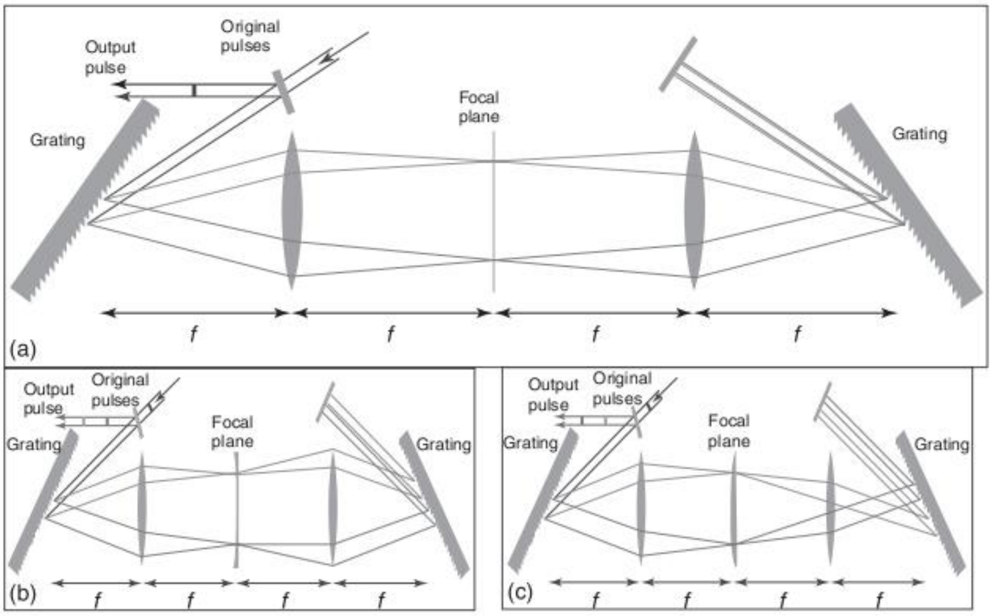

Figure 1(a) Laser pulse shaping fundamental optical geometries, (b) positive chirped and (c) negative chirped shapes.

Objectives:

The objective of the current research is to investigate the effect of a laser beam on a specimen made from composite material. The detailed objectives are:

- CAD modeling of the composite specimen using Creo design software.
- Transient thermal analysis of CFRP specimen using ANSYS
- Transient thermal analysis of GFRP specimen using ANSYS
- Transient thermal analysis of PMMA specimen using ANSYS
- Transient thermal analysis of structural steel specimen using ANSYS
- "Laser" or "laser technology" is the cleanest light produced by scientists. Simplifying, the term "laser" means "light amplification by stimulated emission radiation" in technical terms. Light waves are increased by promoting the emission of light waves. There are a variety of ways to use laser energy depending on the intended use. Lasers can now be used in a broad range of medicinal, surgical, & ophthalmic purposes. Aside from that, it's also employed in the treatments of cancer & homeostatic hemorrhage. Lasers used in medical applications also include a CO_2 laser and an argon laser, among others. Telecommunications experts say that lasers are often utilized to carry messages into devices, such as phones & computers, via optical fibers[1].
- Using a laser to melt materials, the laser cutter creates a cut edge. While it was originally designed for industrial manufacture, it is today found in schools, small enterprises, the architectural industry, and even by those who just want to play around in their spare time. Optics are most typically used to guide the high-power laser's output for laser cutting. Laser optics and computer numerical control (CNC) have been utilized to direct any material or laser beam created. Motion control systems are used by professional laser cutters to follow a pattern to be cut into raw material. The laser beam is concentrated on a particular region of the substance & enables it to either evaporate out, melt, burn, or otherwise degrade in this method.
- Laser cutting is widely utilized in industry to produce complicated forms with tight tolerances. Laser cutting provides many benefits over traditional cutting, including a smaller heat impacted zone, more accuracy, the ability to process without physical touch, as well as a shorter processing time. Laser cutting is being used by manufacturers to improve both the quality & the production of their products. Choice of suitable laser cutting factors like laser power, laser beam diameter, & cutting speed has a significant effect on productivity and quality. Matter & laser cutting parameters interact thermally and mechanically throughout the laser cutting process. HAZ is a term used to describe the area of the base material where heat created during laser cutting has altered the microstructure & mechanical characteristics, but the material itself has not yet melted. This shift in the area surrounding the cut surface is caused by heat created by the laser cutting process and then cooled. Fatigue resistance, surface cracking, & deformation may all occur in HAZ. To reduce heat impacted zones, it is important to pick the correct laser cutting settings[3].

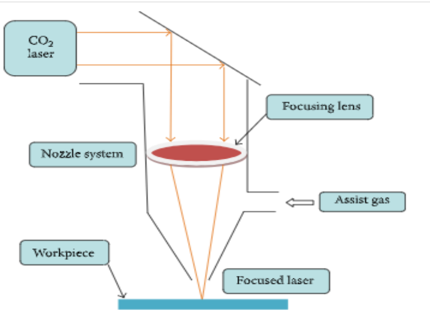

Figure 2: Experimental Laser Cutting Configuration

METHODOLOGY

Methodology Flow Chart

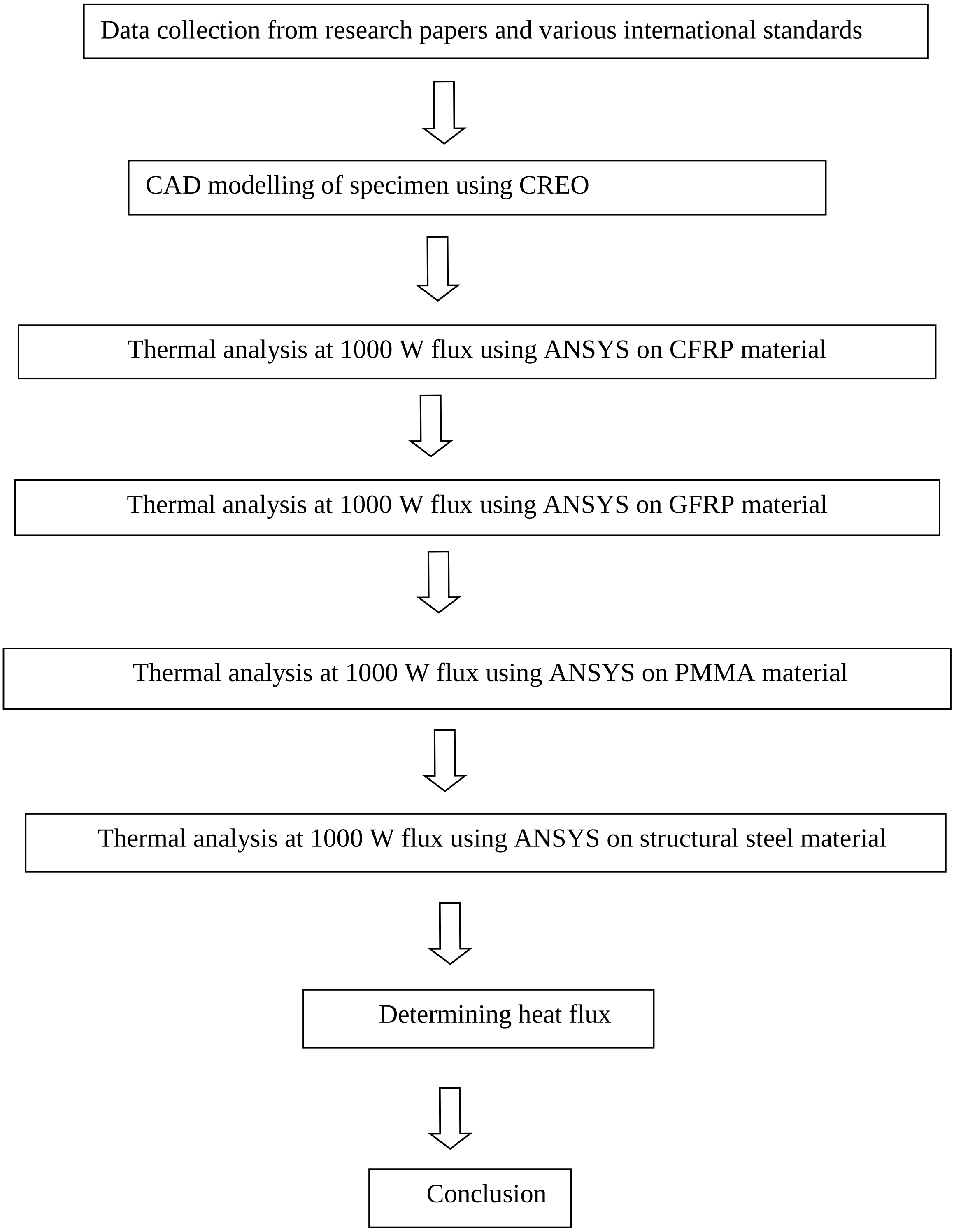

Figure 3: Methodology flowchart

CAD Modelling

The specimen model is generated in Creo design software. This software is parametric and is specially meant for 3D cad modeling. The model is developed and converted into an integrated graphics file format (.iges). This file is imported intothe ANSYS design modeler and checked for surface patches and other geometric errors as shown in figure 4.2 below. The dimensions of the specimen are 50mm * 25mm. The laser beam passes through colored slices in mid-portion.

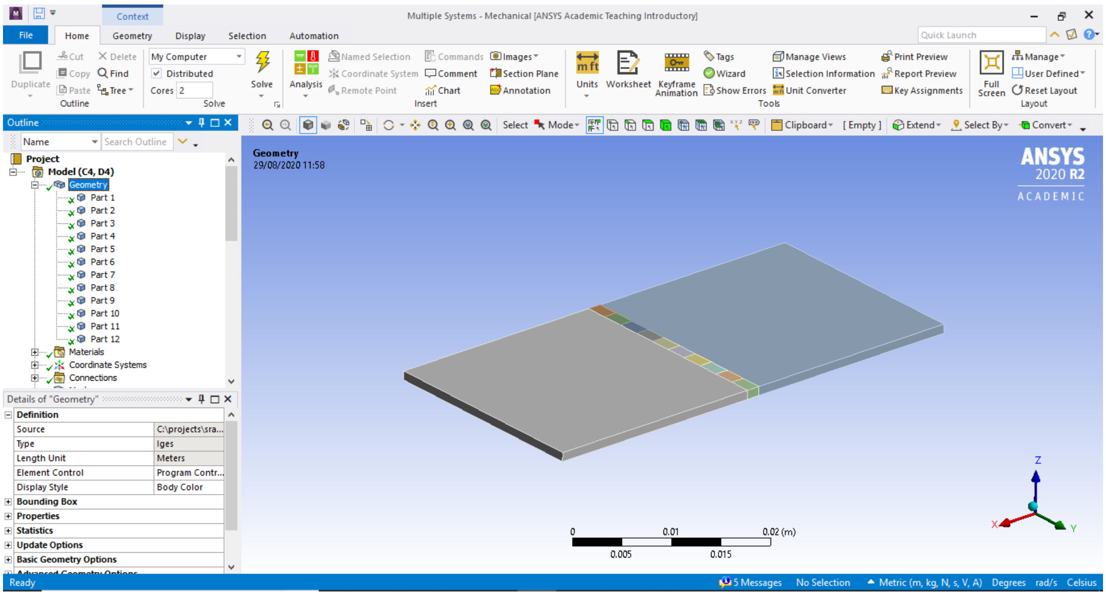

Figure 4: CAD model of the specimen

Meshing

The CAD model is meshed using hexahedral elements with fine sizing. Inflation high, size function adaptive, span angle coarse. The number of elements formulated is 3880 and the number of nodes formulated is 22856.

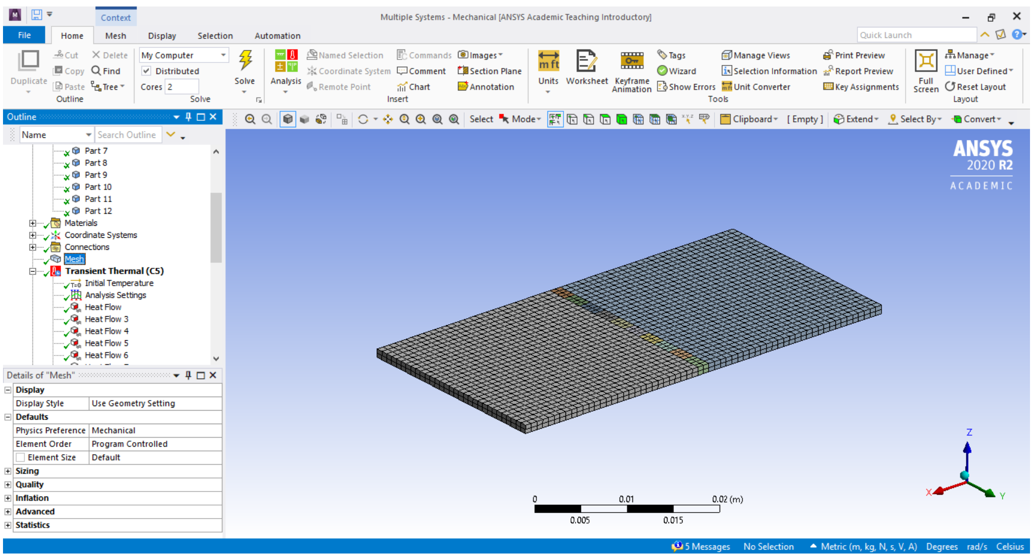

Figure 5: Meshed model of the specimen

Loads and Boundary Conditions

Thermal flux of 1000W magnitude is applied to different segments. The analysis is time-dependent and thermal flux is shifted to the next segment in subsequent time intervals. The heat flux boundary condition is shown in figure 4.3 below. The analysis is performed for 10 counter secs under transient state thermal analysis.

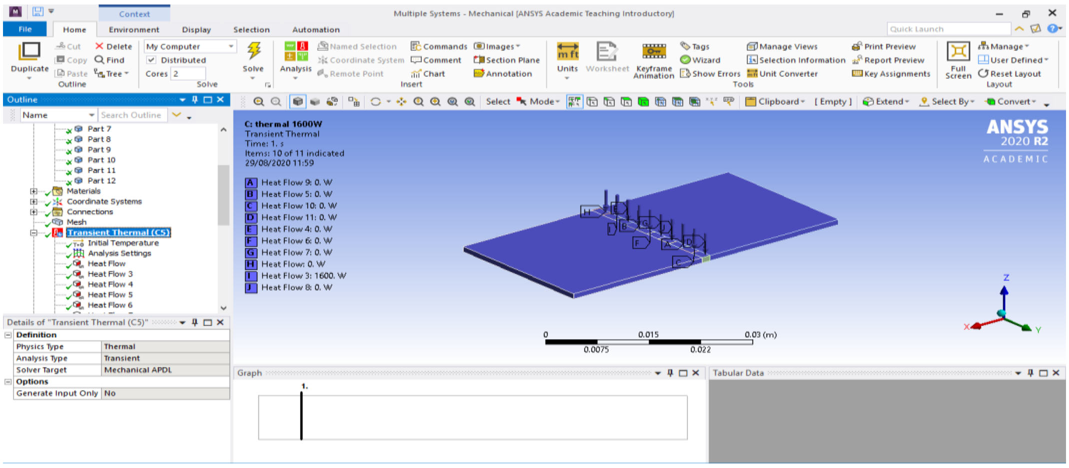

Figure 6 : Thermal Flux boundary condition

Solution Stage

The software carries out matrix formulation, matrix multiplication, and inversions. The global stiffness matrix is formulated and results are carried out at each node and results are interpolated for the entire element edge length.

Post Processing Stage

In this stage contour plots of temperature are plotted at different time intervals and segments as shown in figure 4.4 below.

Analytical Model

For developing an analytical model one of the key assumptions is the homogenous material of the workpiece and Sheetmetal. The gaussian surface model of the laser beam which is supposed to be uniform across Z direction is gen by.

$$\frac{\partial}{\partial x}\left(kx\frac{\partial T}{\partial x}\right)+\frac{\partial}{\partial y}\left(ky\frac{\partial T}{\partial y}\right)+\frac{\partial}{\partial z}\left(kz\frac{\partial T}{\partial z}\right)+q(x\,,y\,,z\,,t)=\rho cp\frac{\partial T}{\partial t}$$

In the above-given equation

T is the temperature in K

t is time in seconds

Kx is thermal conductivity along the x-direction

Ky is thermal conductivity along the y-direction

Kz is thermal conductivity along the z-direction

cp is the specific heat

B. Heat Input

The radially symmetric laser has a Gaussian heat flux profile and 'R' as a function of the amount of heat flux is given by

$$q(R) = \begin{cases} \frac{2P}{\pi r^2} ex\left(-2\frac{R^2}{r^2}\right) & For \quad R \leq r \\ 0 & For \quad R > r \end{cases}$$

Here P is the laser power

R is the radial distance from a beam in m

C. Boundary Condition

The external heat convection (qc) of the workpiece is provided by

$qc = hc\,(T_S.W_T)$

where hc is the convection heat transfer coefficient W/m2-K, and is the ambient temperature. Radiation Heat Transfer It is possible to give the heat loss that is carried from the work piece's surfaces to a lower temperature in the environment through radiation (qr) given by

$qr = \sigma T_S.W - Tamb$

where is the emissivity,

σ is the Stefan-Boltmann constant (5.67 × 10-8 W/m2-K4),

T_S is surface temperature and

Tamb is ambiance temperature.

Thermal Analysis at 1000W power at 2.5mm/sec using CFRP material

Thermal analysis is conducted on cast iron specimens using ANSYS and temperature contours are plotted. The analysis is conducted using a 1000W laser which is applied in the form of heat flux. The analysis is carried out for 10 secs and divided into 10 load steps. In each load step, the thermal flux moves on to the next segment.

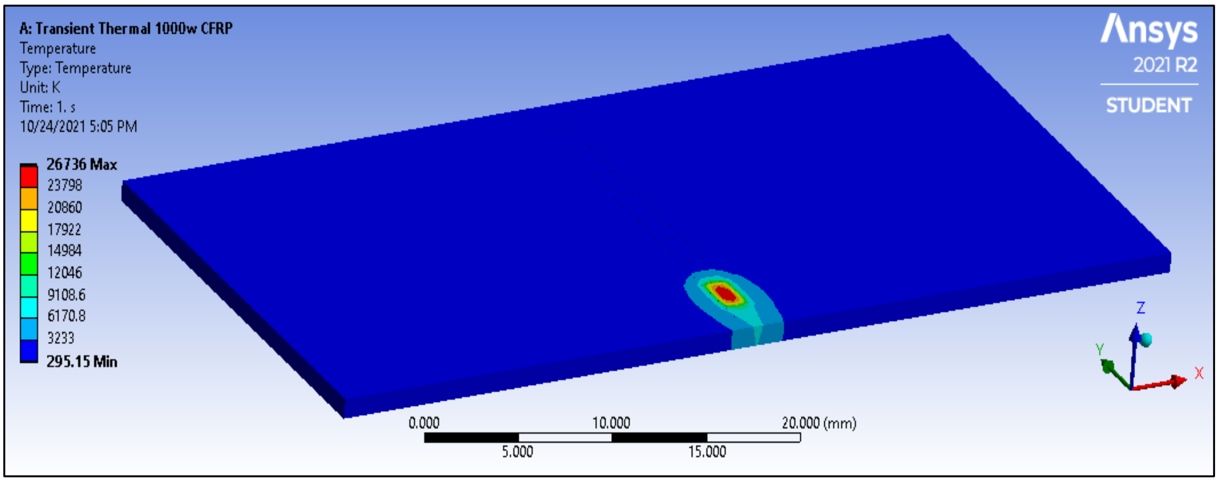

Figure 6: Temperature plot at 1 sec

Figure 6above shows the temperature plot at 1 sec after laser cutting operation. The maximum temperature is 26736°C and the minimum temperature is 3233°C. The temperature reduces as we move away from the cutting zone depicted by red color to light blue color.

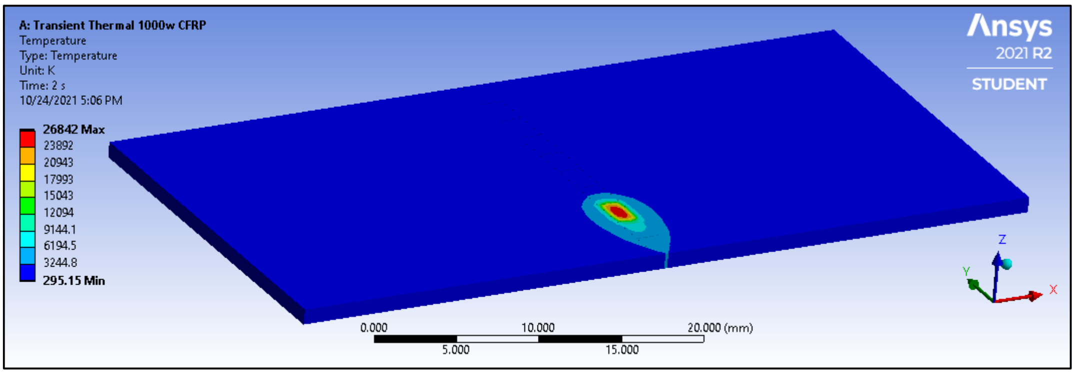

Figure 7: Temperature plot at 2 secs

Figure 7 above shows the temperature plot at 2 secs after laser cutting operation. The maximum temperature is 26842°C and the minimum temperature is 3244.8°C. The temperature reduces as we move away from the cutting zone depicted by red color to light blue color.

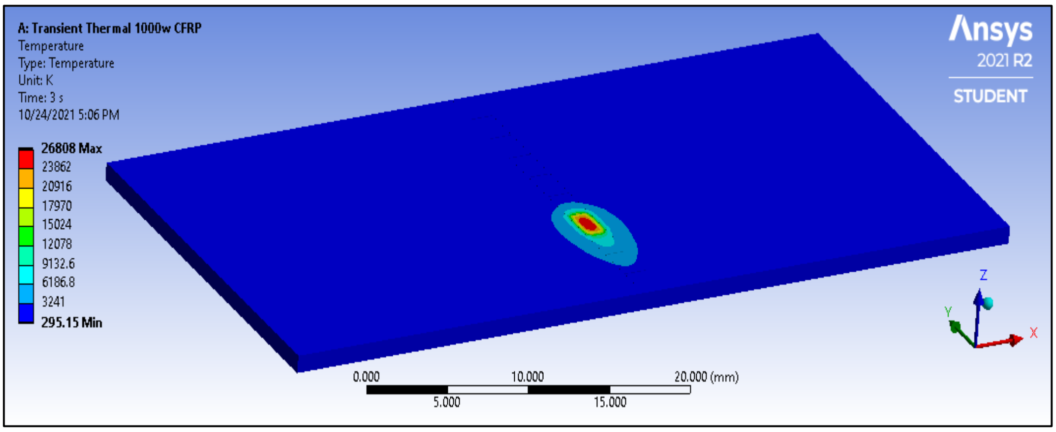

Figure 8: Temperature plot at 3 secs

Figure 8 above shows the temperature plot at 3 secs after laser cutting operation. The maximum temperature is 26808°C and the minimum temperature is 3241°C. The temperature reduces as we move away from the cutting zone depicted by red color to light blue color.

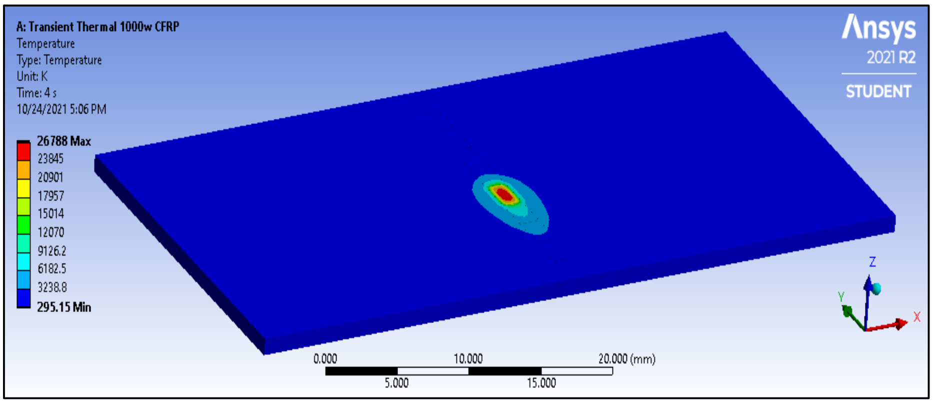

Figure 9: Temperature plot at 4 secs

Figure 9 above shows the temperature plot at 4 secs after laser cutting operation. The maximum temperature is 26788°C and the minimum temperature is 3238.8°C.

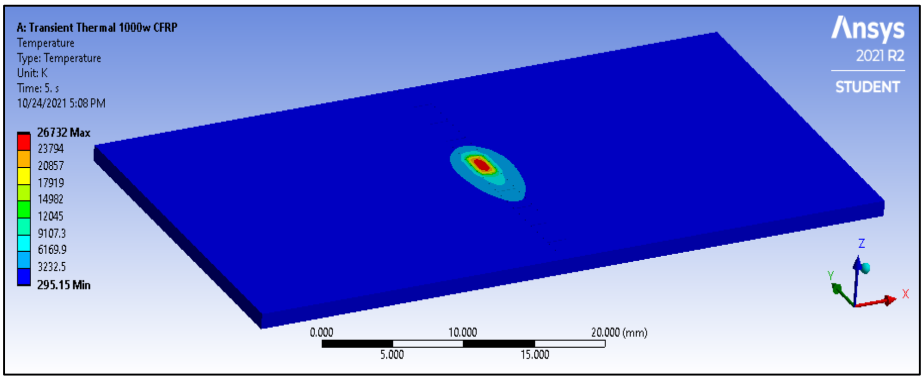

Figure 10: Temperature plot at 5 secs

Figure 10 above shows the temperature plot at 5 secs after laser cutting operation. The maximum temperature is 26732^{o}C and the minimum temperature is 3232.5^{o}C.

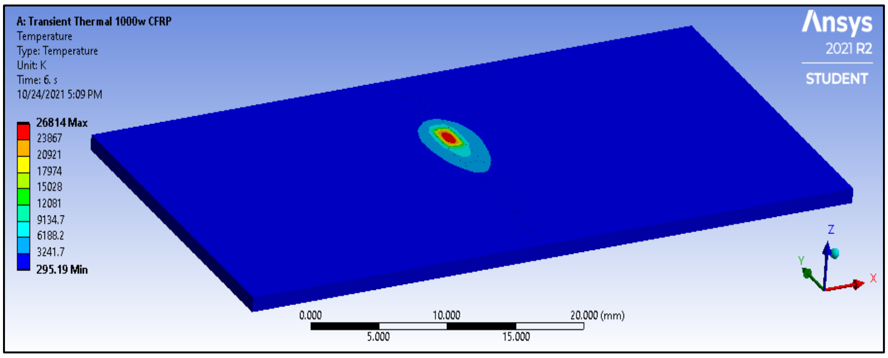

Figure 11: Temperature plot at 6 secs

Figure 11above shows the temperature plot at 6 secs after laser cutting operation. The maximum temperature is 26814 ^{o}C and the minimum temperature is 3241.7 ^{o}C. The temperature reduces as we move away from the cutting zone depicted by red color to light blue color.

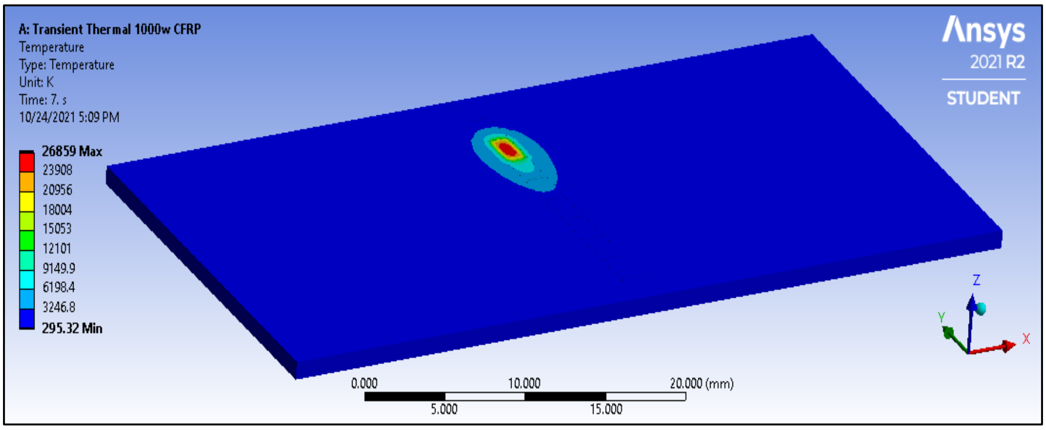

Figure 12 : Temperature plot at 7 secs

Figure 12 above shows the temperature plot at 7 secs after laser cutting operation. The maximum temperature is 26859^{o}C and the minimum temperature is 3246.8 ^{o}C. The temperature reduces as we move away from the cutting zone depicted by red color to light blue color.

Figure 5.13 above shows the temperature plot at 10 secs after laser cutting operation. The maximum temperature is 6145.1 ^{o}C and the minimum temperature is 948.31 ^{o}C. The temperature reduces as we move away from the cutting zone depicted by red color to light blue color.

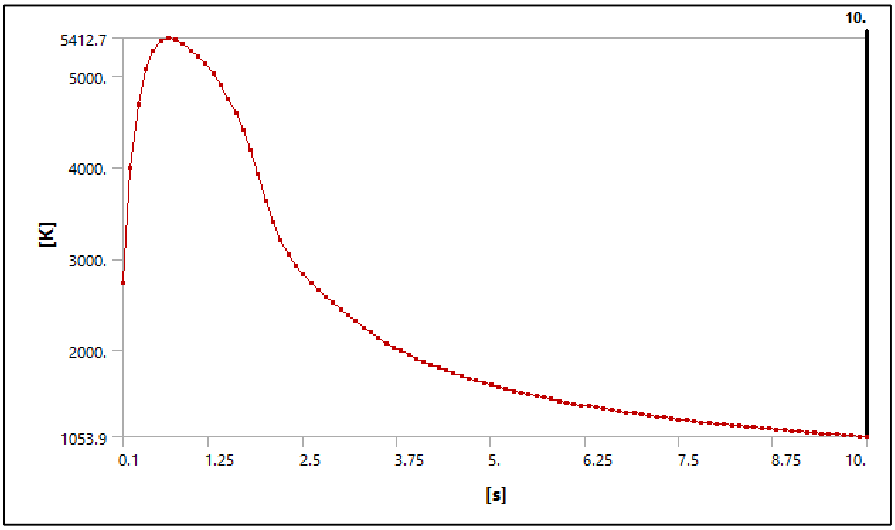

Figure 13: Temperature plot at 1mm distance

Figure 14 shows the temperature-time curve at a point 1mm away from the cutting zone which shows an increase in temperature up to 5412.7^{o}C and reduces to 1053.9^{o}C

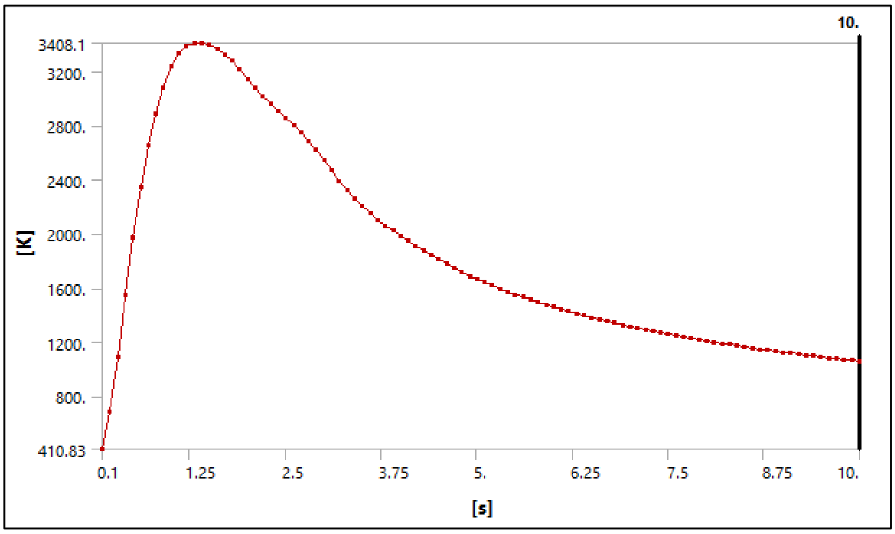

Figure 5.14 Temperature plot at 2mm distance

CONCLUSION

The FEA is a viable tool in determining the thermal characteristics of the composite material specimen on which laser beam is incident. The use of computer simulation can significantly reduce time and cost as against experimental techniques. The transient thermal analysis is conducted on a thin specimen made of composite materials i.e. CFRP, GFRP, PMMA, and structural steel. The temperature plot along with thermal stresses are determined. The detailed results areas:

1. The temperature distribution at the location of laser beam incidence is obtained.
2. The kerf width and HAZ are obtained for all the specimens i.e. CFRP, GFRP, PMMA, and structural steel.
3. The HAZ is highest for steel material and is minimum for PMMA and GFRP. The HAZ for PMMA and GFRP is limited to kerf width.

4. For CFRP material, the maximum temperature obtained at 1mm distance from laser beam incident is 5412.7K, and the maximum temperature at 2mm distance from laser beam incident in 3408.1K.
5. For structural steel, the maximum temperature obtained at 1mm distance from laser beam incident is 3977.3K, and the maximum temperature at 2mm distance from laser beam incident in 1257.6K.

REFERENCES

[1] T. Muangpool and S. Pullteap, “Reviews on laser cutting technology for industrial applications,” no. November, p. 34, 2018, doi: 10.1117/12.2300955.

[2] A. M. Sifullah, Y. Nukman, M. A. Hassan, and A. Hossain, “Finite element analysis of fusion laser cutting on stainless steel-304,” *ARPN J. Eng. Appl. Sci.*, vol. 11, no. 1, pp. 181–189, 2016.

[3] I. Miraoui, M. Boujelbene, and M. Zaied, “High-power laser cutting of steel plates: Heat affected zone analysis,” *Adv. Mater. Sci. Eng.*, vol. 2016, 2016, doi: 10.1155/2016/1242565.

[4] Shane, “5 Applications of Laser Technology in Industrial Production,” *Machine MFG*, 2022. https://www.machinemfg.com/laser-technology-applications/.

[5] E. K. CENTER., “How does the laser process work?,” *ESAB KNOWLEDGE CENTER.*, 2021. https://www.esabna.com/us/en/education/blog/laser-cutting-process.cfm/.

[6] F. Element and A. Using, “Finite Element Analysis Using ANSYS.”

[7] I. E. Reporting, “The Advantages of the Finite Element Method,” *IEEE Innovation*, 2022. https://innovationatwork.ieee.org/the-advantages-of-fem/.

[8] prashantsaini Shahanwazhavale, “What are the advantages and disadvantages of Finite element method.,” *Ques10*. .

[9] sanket shing ote Shaha nwaz havale, “Applications of Finite Element Method,” *Ques10es10*, 2019. https://www.ques10.com/p/23385/explain-the-application-of-fea-in-various-fields/#:~:text=Geotechnical engineering%3A FEM applications include,and dynamic soil structure interaction%5C.

[10] D. T. Academy, “Introduction to Ansys,” *DesignTech system*, 2015. https://www.designtechcadacademy.com/knowledge-base/ansys-software#:~:text=Ansys has been founded in,biomedical and other industrial sectors%5C.

[11] R. Potluri, “ANSYS Training: A Easy Introduction with Applications,” *Udemy*, 2021. https://www.udemy.com/course/fea-with-ansys-workbench/.

[12] I. OZEN ENGINEERING, “ANSYS ADVANTAGES,” *OZEN ENGINEERING, INC.*, 2022. https://www.ozeninc.com/about-ansys/ansys-advantages/#:~:text=Ansys provides you with the,within your company’s user community%5C.

[13] ANSYS, “Applications of ANSYS,” *ANSYS, Inc*, 2022. https://www.ansys.com/en-in/applications%5C.

[14] D. Li, S. Hu, J. Shen, H. Zhang, and X. Bu, “Microstructure and Mechanical Properties of Laser-Welded Joints of Ti-22Al-25Nb / TA15 Dissimilar Titanium Alloys,” *J. Mater. Eng. Perform.*, vol. 25, no. 5, pp. 1880–1888, 2016, doi: 10.1007/s11665-016-2025-4.